Second International Conference on CFD in the Minerals and Process Industries
CSIRO, Melbourne, Australia
6-8 December 1999

DEM SIMULATION OF CHAR COMBUSTION IN A FLUIDIZED BED

Degang RONG and Masayuki HORIO

Department of Chemical Engineering, BASE,
Tokyo University of Agriculture and Technology
Koganei, Tokyo 184-8588 JAPAN

ABSTRACT

A numerical study was conducted based on the discrete element method (DEM) to analyse the thermodynamic characteristics and NO_x emission of burning chars in a fluidized bed. The fluctuations of char particle temperature were investigated taking into account the effects of particle-particle heat conduction, particle-gas heat convection, radiation and combustion. Calculated results show that the maximum temperature of char particles is about $50 \pm 5°C$ higher than the average bed temperature, which is determined by the oxygen concentration nearby and the heat transfer properties of their surrounding gas and particles. NO emission is found to be greatly affected by the temperature of burning char particles.

NOMENCLATURE

A_p particle surface area (both for char and inert particles), m^2
A_{pc} surface area of a char particle, m^2
C_d drag coefficient,
C_i concentration of gas species i , i is O_2, CO_2 and NO respectively, kg/m^3
C_{NO} concentration of NO in a cell, kg/m^3
C^s_{NO} concentration of NO near the char surface, kg/m^3
C_{O_2} concentration of O_2 in a cell, kg/m^3
C_p heat capacity of particle (both for char and inert particle, J/(kJ K)
C_{pg} heat capacity of gas, J/(kJ K)
d_c diameter of char particle, m
d_p particle diameter (both for char and inert particles), m
$\vec{d}_n$ particle displacement in normal direction, m
D_{g1} diffusion coefficient of O_2 in air, m^2/s
D_{g2} diffusion coefficient of NO in air, m^2/s
$\vec{d}_t$ particle displacement in tangential direction, m
e restitution coefficient,
$\vec{F}_c$ force acting on a particle by collision to another particle, N
$\vec{F}_{cn}$ collision force in normal direction, N
$\vec{F}_{ct}$ collision force in tangential direction, N
$\vec{F}_f$ force acting on a particle by fluid drag force, N
$\vec{F}_g$ force acting on a particle by gravity, N
g gravity, m/s^2
h_p heat transfer coefficient, J/(m^{2}s)
I inertia moment of the particle, kgm^2
k spring constant, N/s
k_C rate constant of reaction (C), m/s
$\bar{k}_C$ overall rate constant for reaction (C), m/s
k_E rate constant for reaction (E), m/s
l_{AB} distance between two particle centers, m
M_N molecular weight of N
M_{NO} molecular weight of NO
m_p particle mass (both for char and inert particles), kg
p gas pressure, Pa
Q_{cd} particle-particle conduction, J/s
Q_{cv} particle-gas heat convection, J/s
Q_{gen} heat generation of a burning char, J/s
Q_{rd} particle-bed radiation, J/s
R universal gas constant
R_C reaction rate of reaction (C), kg/s
R_D reaction rate of reaction (D), kg/s
R_E reaction rate of reaction (E), kg/s
r particle radius (both for char and inert particles), m
T particle temperature (both for char and inert particles), K
T_b average bed temperature, K
T_g gas temperature, K
T_{pc} temperature of a char particle, K
T_{pi} temperature of inert particle, K
u_g gas velocity in a cell, m/s
u_x gas velocity in x direction, m/s
u_y gas velocity in y direction, m/s
v particle velocity (both for char and inert particles), m/s
$\dot{\vec{v}}$ particle acceleration, m/s^2
$\vec{v}_n$ particle velocity in normal direction, m/s
$\vec{v}_t$ particle velocity in tangential direction, m/s
x_N mass ratio of nitrogen and oxygen components in the char particle,
Δx width of a cell, m
Δy height of a cell, m
β inter-phase momentum transfer coefficient, kg/(m^{3}s)
δ gas layer thickness (0.5 d_p), m
ε voidage fraction, [-]

η coefficient of viscous dissipation, [-]
λ_g gas conductivity, W/(mK)
μ gas viscosity, Pa.S
μ_f friction coefficient, [-]
ρ_g gas density, kg/m^3
σ Stefan-Boltzmann constant
τ time, s
$\dot{\omega}$ angular acceleration, 1/s^2

INTRODUCTION

Initiated by Avedesian and Davidson (1973) a current body of research was formed on solid fuel combustion including some monumental papers, e.g. Ross and Davidson (1981), La-Nauze and Jung (1983) and Prins (1986). Through the above work we now understand that the combustion of solid fuel is greatly influenced by fluidized bed hydrodynamics via oxygen supply and bed to fuel heat transfer.

The behavior of burning char particles in a fluidized bed is one of the main topics in this research field. During the period of combustion, char particles move from side to side in a fluidized bed and their temperatures fluctuate due to the changes of oxygen concentration and char-to-bed heat transfer. Since the emission of NO_x and other toxic compounds in a fluidized bed depends strongly on such a combustion process, the current work is of significant importance.

Nowadays with the rapid development of computer technology and the numerical tool - the DEM (discrete element method), a new era of research on gas-solid heterogeneous reaction systems is about to come. The DEM simulation provides a new way to analyze the gas-solid fluidized bed processes because it can predict individual particle behavior as well as the local gas flow information, although there are still some simplifications.

The objective of the present work is to develop a DEM based model for char combustion and to provide data from the numerical experiment for microscopic combustion behavior of char particles.

THEORY

A schematic representation of phenomena is given as: 20 char particles with diameter of 1mm are spread randomly into a fluidized bed (60mm in width, 120mm in height and 1mm in thickness); the char particles react with their surrounding gases while heat exchange occurs between particle-particle, particle-gas and gas-gas; the initial temperatures of char particles, bed material and fluidizing gases are $850°C$; the behavior of char combustion in the initial 4.1s were simulated.

The DEM model of char combustion in a fluidized bed contains three sub-models, one is the hydrodynamics, another is the combustion/reaction and the third is the heat and mass transfer.

Hydrodynamics

The hydrodynamic sub-model consists of two parts: particle interaction and motion, and fluid motion.

Particle-particle interaction and particle motion

The discrete particle method was applied here to calculate the particle-particle interaction in a fluidized bed. Based on the "soft sphere" assumption initially proposed by Tsuji et al. (1993), each collision particle is assumed to have a normal and tangential springs and dash pots together with a tangential slider. During a collision the contacting area and repulsive force change with the displacement of particles. The calculation of the particle-particle contact duration and contact area provides the fundamental of particle-particle heat transfer discussed later in this paper. The particle motion is dependent on Newton's second law:

$$m_p\dot{\vec{v}} = \sum \vec{F}_c + \vec{F}_f + \vec{F}_g \quad (1)$$

where $\vec{F}_c$, $\vec{F}_f$, and $\vec{F}_g$ are the forces acting on a particle caused by collision, fluid drag force and gravity, respectively; m_p is the particle mass and $\dot{\vec{v}}$ is the acceleration of the particle.

The particle-particle collision force $\vec{F}_c$ is based on the soft sphere approach, which can further be divided into normal and tangential components: $\vec{F}_{cn}$ and $\vec{F}_{ct}$,

$$\vec{F}_{cn} = -k\vec{d}_n - \eta\vec{v}_n \quad (2)$$

$$\vec{F}_{ct} = -k\vec{d}_t - \eta\vec{v}_t \qquad (|\vec{F}_{ct}| < \mu_f|\vec{F}_{cn}|) \quad (3)$$

$$\vec{F}_{ct} = -\mu_f|\vec{F}_{cn}|\cdot(\frac{\vec{v}_t}{|\vec{v}_t|}) \qquad (|\vec{F}_{ct}| \geq \mu_f|\vec{F}_{cn}|) \quad (4)$$

where $\vec{d}_n$ and $\vec{d}_t$ are the particle displacements in normal and tangential directions, respectively; k is the spring constant; $\vec{v}_n$ and $\vec{v}_t$ are the particle velocities in normal and tangential directions; η is the coefficient of viscous dissipation; μ_f is the friction coefficient. Among them, parameters k, η and μ_f have to be chosen. The spring constant k used in this work is 2.22x10^{5}N/m, the friction coefficient μ_f is assumed to be 0.3 and η is determined by the restitution coefficient *e* (*e*=0.9):

$$\eta = 2\ln e\sqrt{\frac{mk}{\pi^2 + \ln^2 e}} \quad (5)$$

The tangential component of collision force acting on a particle, $\vec{F}_{ct}$, causes particle rotation. This rotation motion can be expressed as:

$$\dot{\omega} = \frac{r_p\sum\vec{F}_{ct}}{I} \quad (6)$$

where I is the inertia moment of a particle, r_p is the particle radius and $\dot{\omega}$ is the angular acceleration.
With respect to the calculation of particle-fluid interaction force, $\vec{F}_f$, it is similar to the treatment by Mikami et al (1998).

Fluid motion

In fluid calculation the Anderson and Jackson(1967)'s volume averaged Navier-Stokes equations were applied:

$$\frac{\partial\varepsilon}{\partial\tau} + \nabla\cdot(\varepsilon u_g) = 0 \quad (7)$$

$$\frac{\partial(\rho_g\varepsilon u_g)}{\partial\tau} + \nabla\cdot(\rho_g\varepsilon u_g u_g) = -\varepsilon\nabla p + \beta(v - u_g) + \varepsilon\rho_g g$$

(8)

where g is the gravity, p is the gas pressure, u_g is the gas velocity, v is the particle velocity, β is the inter-phase momentum transfer coefficient, ε is the voidage fraction and ρ_g is the gas density.

For β, when the void fraction (porosity) $\varepsilon < 0.8$, it can be obtained from Ergun equation,

$$\beta = 150\frac{(1-\varepsilon)^2}{\varepsilon}\frac{\mu}{d_p^2} + 1.75(1-\varepsilon)\frac{\rho_g}{d_p}\left|u_g - v\right| \qquad (9)$$

where d_p is the particle diameter and μ is the gas viscosity.

When $\varepsilon \geq 0.8$, the Wen-Yu (1966)'s correlation was adopted:

$$\beta = \frac{3}{4}C_d\frac{(1-\varepsilon)\varepsilon}{d_p}\rho_g\left|u_g - v\right|\varepsilon^{-2.65} \qquad (10)$$

where the drag coefficient C_d is a function of the particle Reynolds number,

$$Re_p = \frac{\left|u_g - v\right|}{\mu}d_p\varepsilon\rho_g \qquad (11)$$

$$\text{and, } C_d = \frac{24}{Re_p}(1+0.15Re_p^{0.687}) \quad (\mathrm{Re}_p < 1000) \qquad (12)$$

$$C_d = 0.44 \quad (\mathrm{Re}_p \geq 1000) \qquad (13)$$

The hydrodynamic sub-model can provide the average gas velocity in a cell as well as the location, the velocity and the contact process of each particle.

Char combustion/reaction

The basic assumptions are as follows:

(a) diameter of char particles keeps constant when burning within the short period – 4.1s;

(b) CO is generated by the reaction of C and O_2 at the particle surface and then CO is further oxidized rapidly to CO_2 near the particle surface. Hence, the overall reaction is expressed by C, O_2 and CO_2;

(c) NO_x (NO) emission is simplified to occur at the particle surface with the consumption of Carbon;

(d) reduction rate of NO is proportional to the NO concentration;

(e) each reaction is of first-order.

(f) the char particle consists of C and N with the weight fraction of N being 2.4%.

Therefore, the main reactions can be expressed as,

$C + 1/2O_2 \rightarrow CO$ (A)

$CO + 1/2O_2 \rightarrow CO_2$ (B)

$C + O_2 \rightarrow CO_2$ (C)

$\text{Char-N} \rightarrow NO$ (D)

$NO + \text{Char} \rightarrow N_2$ (E)

where, reaction (C) is the overall reaction of reactions (A) and (B).

The reaction rates R_i of reactions (C), (D) and (E) are:

$$R_C = \bar{k}_C A_{pc} C_{O_2} \qquad (14)$$

$$R_D = x_N R_C \cdot M_{NO} / M_N \qquad (15)$$

$$R_E = k_E A_c C_{NO}^S \qquad (16)$$

where A_{pc} is the surface area of a char particle; C_{O_2} is the concentration of O_2 in a cell; C_{NO}^S is the NO concentration near the particle surface; $\bar{k}_C$ is the overall rate constant for reactions (C); k_E is the rate constant of reaction (E); M_{NO} and M_N are the molecular weight of NO and N, respectively; x_N is the mass ratio of nitrogen and oxygen components in the char particle.

The overall rate constant $\bar{k}_C$ is determined by:

$$\bar{k}_C = 1/(1/k_C + d_c / ShD_{g1}) \qquad (17)$$

$$Sh = 2(1+0.30Re_c^{0.5}Sc_c^{0.33}) \qquad (18)$$

$$Re_c = d_c u_g \rho_g / \mu \qquad (19)$$

$$Sc_c = \mu / (\rho_g D_{g1}) \qquad (20)$$

where d_c is the diameter of char particle; D_{g1} is the diffusion coefficient of O_2 in air; k_C is the rate constant of reaction (C); u_g is the gas velocity in the cell; μ is the gas viscosity; ρ_g is the gas density.

Among them, the rate constant of reaction (C) k_C was approximated by the rate constant of reaction (A) given by Field et al.(1967):

$$k_C = 595T_{pc}\exp(-149227/RT_{pc}) \qquad (21)$$

in which T_{pc} is the temperature of a char particle and R is the universal constant.

The O_2 consumption rate R_{O2} for a burning char is:

$$R_{O2} = R_C(32/12) \qquad (22)$$

The CO_2 generation rate R_{CO2} for a burning char is:

$$R_{CO2} = R_C(44/12) \qquad (23)$$

The NO accumulating rate R_{NO} for a burning char can be calculated by:

$$R_{NO} = \frac{1}{1/k_E + d_c / ShD_{g2}}\left(R_D / k_E - A_{pc}C_{NO}\right) \qquad (24)$$

$$k_E = 1.3\times10^5\exp(-34000/RT_{pc}) \qquad (25)$$

where C_{NO} is the concentration of NO in the cell; D_{g2} is the diffusion coefficient of NO in air; k_E is the rate constant of reaction (E), which is similar to that used by Horio et al.(1979).

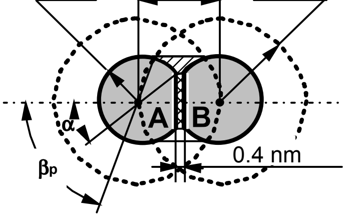

Figure 1: Assumption of particle-particle heat transfer

Heat and mass transfer

Heat transfer of particles

For a fluidized bed without immersed

heat exchangers, the heat transfer of particles may divided into three parts: particle-gas heat convection Q_{cv}; particle-bed radiation Q_{rd}; particle-particle conduction Q_{cd}.

Therefore, the heat balance for a char particle at temperature T_{pc} or an inert particle at temperature T_{pi} can be written in a general form:

$$m_p C_p dT_p / d\tau = Q_{gen} - (Q_{cv} + Q_{rd} + Q_{cd}) \quad (26)$$

where C_p is the particle heat capacity; m_p is the particle mass; Q_{gen} is the heat generation of a particle; T_p is the particle temperature.

For the calculation of particle-gas heat convection Q_{cv}, Ranz's (1952) correlation was adopted to determine the heat transfer coefficient h_p:

$$Q_{cv} = h_p A_p (T_p - T_g) \quad (27)$$

$$h_p = Nu_p \lambda_g / d_p \quad (28)$$

$$Nu_p = 2 + 0.6 Re_p^{1/2} Pr^{1/3} \quad (29)$$

where A_p is the particle surface area; d_p is the particle diameter; T_g is the gas temperature; λ_g is the gas conductivity.

The particle-bed radiation Q_{rd} is given by:

$$Q_{rd} = \sigma \varepsilon_e A_p (T_p^4 - T_b^4) \quad (30)$$

where T_b is the average bed temperature approximated by averaging the particle temperatures; σ is the Stefan-Boltzmann constant; ε_e is the particle emissivity of radiation, which was assumed to be 0.85.

With respect to the particle-particle heat conduction Q_{cd}, previous researchers usually neglected this part but now we attempt to take into account this problem by using DEM model.

The mechanism of particle-particle conduction is shown in Fig.1. As illustrated, each particle is assumed to be surrounded by a gas layer with thickness δ of $0.5d_p$ (here $d_p = 1mm$). When the distance l_{AB} between particle A and particle B is greater than $1.5d_p$, particle-particle heat conduction is not considered. As the two particles approach each other and the distance l_{AB} is less than $1.5d_p$, the particle-particle heat conduction occurs. In this case, when l_{AB} is greater than d_p, the particle-particle heat transfer is supposed to be heat absorption and release through the interstitial gas layer; when l_{AB} is less than d_p, heat conduction through the particle-particle contact point is taken into account as well as that through the gas layer. Further assumptions are:

(a) the contacting surface is smooth and perpendicular to the center line of the relevant contacting particles;
(b) the area of contacting surface is based on the particle overlap based on DEM model;
(c) there is a minimum gas interval between the contacting surface, which is $4 \times 10^{-10} m$;
(d) the heat transfer through a contacting point (surface) is based on the heat conduction through the gas interval;
(e) the heat conduction through the gas layer occurs at the direction parallel to the center line of the relevant two particles;
(f) the heat transfer resistance inside the particle is neglected.

Accordingly, the particle-particle heat conduction Q_{cd} can be written:

$$Q_{cd} = -\lambda_g \frac{T_p(A) - T_p(B)}{4 \times 10^{-10}} \pi (r \sin \beta_p)^2 - \lambda_g (T_p(A) - T_p(B)) \int_{\beta_p}^{\alpha} \frac{2\pi r \sin\theta}{l_{AB} - 2r\cos\theta} d(r\sin\theta) \quad (l_{AB} \le d_p) \quad (31)$$

$$Q_{cd} = -\lambda_g (T_p(A) - T_p(B)) \int_0^{\alpha} \frac{2\pi r \sin\theta}{l_{AB} - 2r\cos\theta} d(r\sin\theta) \quad (d_p \le l_{AB} \le 1.5d_p) \quad (32)$$

where r is particle radius; $T_p(A)$ and $T_p(B)$ are the temperatures of particle A and B, respectively; α is the angle relevant to the intersection point determined by the outline of particle A and the gas layer of particle B (cf. Fig.1); β_p is relevant to the overlap of the two particles. Angle α and β_p are given as:

$$\alpha = \cos^{-1}\left(\frac{l_{AB}^2 + r^2 - (r+\delta)^2}{2rl_{AB}}\right) \quad (33)$$

$$\beta_p = \cos^{-1}\left(\frac{l_{AB}^2 + r^2 - r^2}{2rl_{AB}}\right) \quad (34)$$

where δ is the thickness of the gas layer and here $\delta = 0.5d_p$.

Heat balance for a fluid cell

Since the thickness of the fluidized bed is equal to the particle diameter, the fluidizing regime is indeed two-dimensional. Hence, the equation of heat balance for a fluid cell can be written:

$$\frac{\partial(\varepsilon T_g)}{\partial \tau} + \frac{\partial(\varepsilon u_x T_g)}{\partial x} + \frac{\partial(\varepsilon u_y T_g)}{\partial y} = \frac{q_{cv} + q_{re}}{\rho_g C_{pg}} \quad (35)$$

with boundary conditions:

$$\frac{\partial T_g}{\partial x} = 0, \quad \text{(for impermeable bed bottom)} \quad (36)$$

$$\frac{\partial T_g}{\partial y} = 0, \quad \text{(for impermeable bed side wall)} \quad (37)$$

where C_{pg} is the heat capacity of gas; q_{cv} is the convection heat transfer from particles to gases in a cell; q_{re} is the heat release of burning particles by the consumption of O_2 and the generation of CO_2 near the particle surface; T_g is the gas temperature; u_x and u_y are the gas velocity components in the x and y direction, respectively; ε is the voidage of the cell; ρ_g is the gas density; τ is time. Among them, q_{cv} and q_{re} are:

$$q_{cv} = \sum Q_{cv} / (\Delta x \Delta y) \quad (38)$$

$$q_{re} = \sum (T_p C_{pg} m_{CO2} - T_g C_{pg} m_{O2}) / (\Delta x \Delta y)$$

$$= \sum (T_p C_{pg} R_C 44/12 - T_g C_{pg} R_C 32/12)/(\Delta x \Delta y) \quad (39)$$

where m_{CO2} is the CO_2 generation rate of a burning particle; m_{O2} is the O_2 consumption rate of a burning particle; Q_{cv} is the heat convection between a single particle and the gas (cf. eqn.19); R_C is the reaction rate of reaction (C); T_g and T_p are the gas and particle temperature, respectively; Δx and Δy are the width and height of the cell, respectively.

Mass balance for gas species in a cell

The mass balance for gas species i (CO_2, O_2 and NO) in a cell is :

$$\frac{\partial(\varepsilon C_i)}{\partial \tau} + \frac{\partial(\varepsilon u_x C_i)}{\partial x} + \frac{\partial(\varepsilon u_y C_i)}{\partial y} = cm_i \quad (40)$$

with boundary conditions:

$$\frac{\partial C_i}{\partial x} = 0, \text{ (for impermeable bed side wall)} \quad (41)$$

$$\frac{\partial C_i}{\partial y} = 0, \text{ (for impermeable bed bottom)} \quad (42)$$

where C_i is the concentration of gas species i in the cell; cm_i is the generation rate of gas species i in the cell:

$$cm_{O2} = -\sum R_{O2}/(\Delta x \Delta y) \quad (43)$$

$$cm_{CO2} = \sum R_{CO2}/(\Delta x \Delta y) \quad (44)$$

$$cm_{NO} = \sum R_{NO}/(\Delta x \Delta y) \quad (45)$$

in which R_{O2}, R_{CO2} and R_{NO} are the generation rates of gas species O_2, CO_2 and NO, respectively.

COMPUTATION CONDITIONS

The simulated fluidized bed is 60×120 mm in width and height, and 1mm in thickness (cf. Fig.1). The particle diameter is 1mm; the numbers of char pariticles and inert particles are 20 and 2000, respectively; the densities of char and inert particles are 1360 and 2520 kg/m^3, respectively; the initial bed temperature is 850^{0}C; the fluidization gas is air of 850^{0}C and the fluidizating velocity is 1.2m/s. For the fluid (gas) calculation, the bed is covered with square cells; each cell is 6×6 mm in width × height.

The computation was done for 4.7s. At the first 0.6s, the bed was fluidized to establish a well fluidization condition. Then, at the moment of 0.6s, 20 particles among the bed were defined to be char particles and the behavior of these char particles were investigated based on the latter 4.1s (from 0.6s – 4.7s).

RESULTS AND DISCUSSION

The calculated snapshots of the fluidization are shown in Fig.2 as "a", "b" and "c" corresponding to different

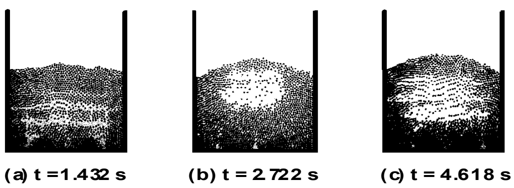

Figure 2 : Fluidization conditions of the bed at moments "a", "b" and "c"

moments, which will be used in the later discussion. In the present simulation, the temperature fluctuations of particles during the calculated 4.1s are recorded.

As shown in Fig.3, the maximum temperatures of those char particles (No.1 – No.4) are $900 \pm 5°C$ which is about $50°C$ higher than the bed temperature. Since the char particle is small, the particle temperature changes fiercely with a frequency of roughly 5-7Hz. To further understand the fluctuation of char temperature, the gas temperature and oxygen concentration around the char No.3 are

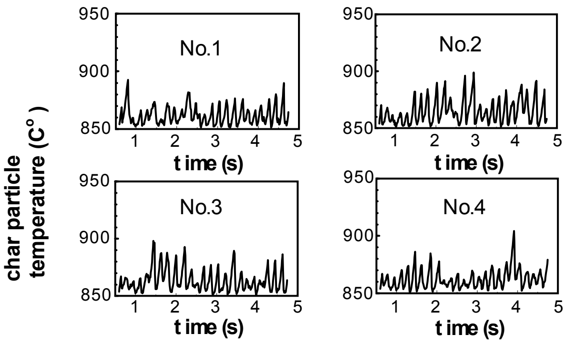

Figure 3 : Fluctuation of char particle temperatures

illustrated in Fig.4.

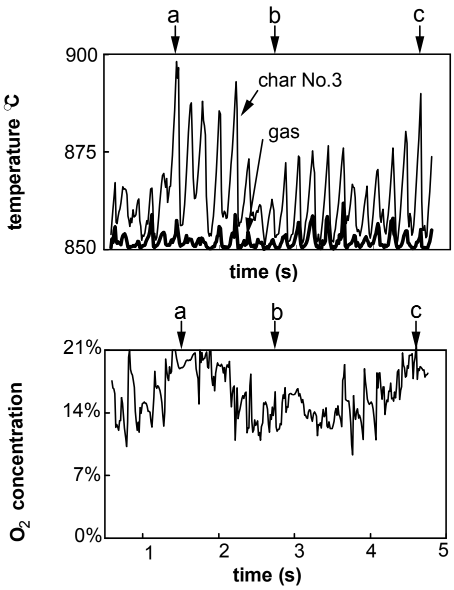

Figure 4: Relationship between char temperature and gas temperature / Oxygen concentration

It can be seen the gas temperature fluctuates with the fluctuation of char temperature and the frequency is about 6Hz.

Also in Fig.4, it can be found the char temperature is deeply affected by the oxygen concentration in gas surrounding the char particles. At the moments of "a", "b" and "c" ("a", "b" and "c" correspond to the moments in Fig.2), the high char temperatures link with high oxygen concentrations (cf. "a", "c") whereas the low temperature links with low oxygen concentration (cf. "b").

Fig.5 shows the situation of particle-particle contacts around char No.3 at moments "a", "b" and "c". It is interesting to find that there is only one particle near the char No.3 at moments "a" and "c" when the char temperatures are high, whereas there is six inert particles surrounding it at moment "b" when the char temperature is low.

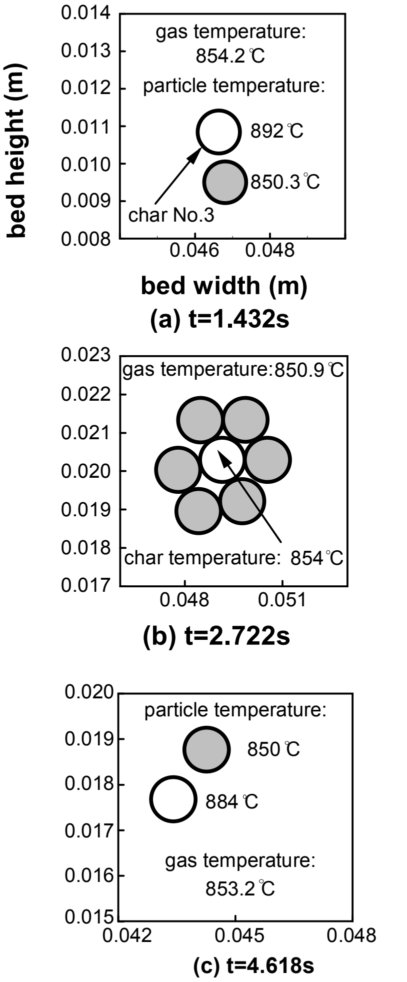

Figure 5 : Situation of char No.3 at moments "a", "b" and "c"

Fig.6 illustrates the NO and O_2 concentration distributions as well as the gas temperature distribution in the bed at moment "a". The NO concentration is extremely low and its local maximum value is roughly 3.7ppm. This is because the char temperatures are as low as $850-900°C$ (cf. Fig. 3) and the weight fraction of char particles in the whole bed is only 0.45%. The oxygen concentration shown in Fig.6 is generally higher especially in the bed center and the bottom area where the local maximum value of oxygen concentration is almost equal to the inlet oxygen concentration 0.21. This is also due to the low concentration of char particles in the bed. The gas temperature distribution indicates that the local maximum gas temperature is about $856-858°C$ at moment "a".

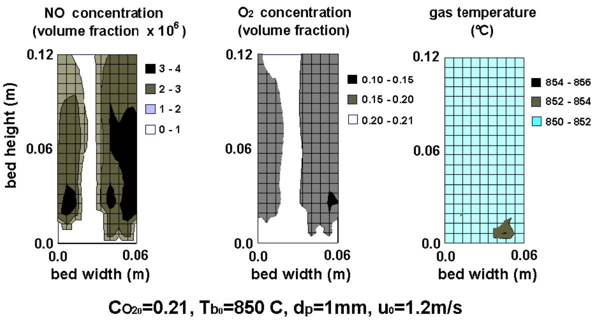

Figure 6 : NO & O_2 concentration and gas temperature in the bed at moment "a" (t= 1.432 s)

CONCLUSION

A mathematical model based on the discrete element method (DEM) has been developed to simulate char combustion in a fluidized bed. The hydrodynamics and heat transfer processes during char combustion were precisely investigated since the parameters of gas were defined in each small cell while the parameters of particle were defined individually for each particle. The temperature fluctuations of char particles were analyzed as well as the NO emission in the bed.

The calculated results illustrated that the char temperature fluctuated at a frequency of 5-7Hz and the maximum char temperature was $50 \pm 5°C$ higher than the average bed temperature. This kind of char temperature fluctuation was deeply affected by the oxygen concentration nearby and the local particle-bed heat transfer because higher char temperature linked with higher oxygen concentration and lower particle-bed heat release.

Also, the calculated results showed that the NO concentration was very low in the bed. The low NO emission was caused by lower temperature of the burning char particles.

REFERENCES

ANDERSON, T. B. and JACKSON, R. (1967) A fluid mechanical description of fluidized beds. *I&EC Fundam.* **6**, 527-539.

AVEDESIAN, M. M. and DAVIDSON, J. F. (1973) Combustion of carbon particles in a fluidized bed. *Trans. Inst. Chem. Engrs.*, **51**,121-131.

FIELD, M. A., GILL, D. W., MORGAN, B. B. and HAWKSLEY, P. G. W. (1967) Combustion of pulverized fuel, BCURA Leatherhead, 1967.

HORIO, M., MORI, S. and MUCHI, I. (1979) A model study for the development of low NO_x fluidized bed coal combustors. *Proceedings of the 3th International Conference on Fluidized Bed Combustion*, ASME, ed Vol. 605-623

LA-NAUZE, R. D. and JUNG, K. (1983) *Proceedings of the 7th International Conference on Fluidized Bed Combustion,* ASME, 1040-1046.

MIKAMI, T., KAMIYA, H. and HORIO, M. (1998) Numerical simulation of cohesive powder behavior in a fluidized bed. *Chem. Engng. Sci.*, **53**, 1927-1940.

PRINS, W. (1986) Ph.D. Thesis, Fluidized bed combustion of single particle. Twente University of Technology. The Netherlands.

RANZ, W. E. and MARSHALL, W. R. (1952) *Chem. Eng. Prog.*, **48**, 141-147.

ROSS, I. B. and DAVIDSON, J. F. (1981) The combustion of carbon particles in a fluidized bed. *Trans IChemE.*, **59**, 108-114.

TSUJI, Y., KAWAGUCHI, T. and TANAKA, T. (1993) Discrete particle simulation of two-dimensional fluidized bed. *Powder Technology.* **77**, 79-87.

WEN, C. Y. and YU, Y. H. (1966) A generalized method for predicting the minimum fluidization velocity. *A.I.Ch.E. J.* **12**, 610-612.

WEN, C. Y. and CHANG, T. M. (1967) Particle-to-particle heat transfer in air-fluidized beds. *Proceedings of the International Symposium on Fluidization,* Eindhoven, 491-506.